YITP–99–4
TU–559
January 1999

Neutralino decays at the CERN LHC

Mihoko M. Nojiri[a] and Youichi Yamada[b]

[a] *YITP, Kyoto University, Kyoto 606-8502, Japan*
[b] *Department of Physics, Tohoku University, Sendai 980-8578, Japan*

Abstract

We study the distribution of lepton pairs from the second lightest neutralino decay $\tilde{\chi}_2^0 \to \tilde{\chi}_1^0 l^+ l^-$. This decay mode is important to measure the mass difference between $\tilde{\chi}_2^0$ and the lightest neutralino $\tilde{\chi}_1^0$, which helps to determine the parameters of the minimal supersymmetric standard model at the CERN LHC. We found that the decay distribution strongly depends on the values of underlying MSSM parameters. For some extreme cases, the amplitude near the end point of the lepton invariant mass distribution can be suppressed so strongly that one needs the information of the whole m_{ll} distribution to extract $m_{\tilde{\chi}_2^0} - m_{\tilde{\chi}_1^0}$. On the other hand, if systematic errors on the acceptance can be controlled, this distribution can be used to constrain slepton masses and the $Z\tilde{\chi}_2^0\tilde{\chi}_1^0$ coupling. Measurements of the velocity distribution of $\tilde{\chi}_2^0$ from samples near the end point of the m_{ll} distribution, and of the asymmetry of the p_T of leptons, would be useful to reduce the systematic errors.

1 Introduction

If supersymmetry is realized in nature, it promises exciting possibilities for future collider physics — the discovery of sparticles. If the scale of supersymmetry breaking is around 1 TeV (as preferred by fine-tuning arguments related to problems in the Higgs sector), many sparticles will be produced at future colliders such as the Fermilab Tevatron upgrade, the CERN Large Hadron Collider (LHC), or future e^+e^- colliders proposed by DESY, KEK, and SLAC. Sparticles produce unique signatures in the detectors and will be discovered quite easily.

It has been pointed out that one cannot only discover those sparticles, but can also study their detailed nature in future e^+e^- colliders. By measuring sparticle masses, production cross sections for a polarized electron beam, and other distributions, we will measure soft supersymmetry breaking mass parameters [1, 2, 3, 4, 5] and prove supersymmetric relations [6]. Studies at future e^+e^- colliders should reveal details of the mechanism to break supersymmetry.

Corresponding studies for the LHC have been performed in [7, 8] in the framework of the minimal supergravity model. These analyses show that a precise determination of the model parameters is possible; the LHC is especially powerful when the gluino decay $\tilde{g} \to b\tilde{b}$ followed by $\tilde{b} \to b\tilde{\chi}_2^0$, $\tilde{\chi}_2^0 \to l^+l^-\tilde{\chi}_1^0$ can be identified by tagging the bottom jets and the hard leptons. One of the key tricks of the studies is the measurement of the end point of the invariant mass distribution of the lepton pair with same flavor and opposite charges. The end point determines the mass difference between the second lightest and the lightest neutralino [9], $m_{\tilde{\chi}_2^0} - m_{\tilde{\chi}_1^0}$. The kinematically constrained nature of the end point samples allows one to reconstruct the decay chains to determine the parameters of minimal supergravity model [7, 8]. At the end, all or some of the parameters in the model would be determined.[1]

However, the minimal supergravity model is not the only model for spontaneous supersymmetry breaking in a phenomenologically consistent manner. Moreover, there are various possibilities even within the supergravity model, as summarized in Ref. [12] for example. Other mechanisms to break supersymmetry (SUSY) are also discussed extensively [11, 13].

Assuming that the LHC can determine all parameters within the minimal supergravity model by looking into some signal distributions, the next

[1] A similar analysis can be done [10] for the parameter dependence of gauge mediated supersymmetry breaking models [11].

question is what we should look into to over-constrain the model, or to determine deviations from the minimal supergravity model. As we mentioned before, studies in this direction have been done in great detail for future e^+e^- colliders. For hadron colliders, such a study would be complicated because more than one SUSY channel can contribute to a particular class of events since different sparticles are simultaneously produced.

In this paper, we discuss the parameter dependence of the distribution of the three body decay $\tilde{\chi}_2^0 \to \tilde{\chi}_1^0 l^+ l^-$. The decay branching ratio depends on parameters in the minimal supersymmetric standard model (MSSM) rather sensitively due to (possibly negative) interference between slepton and Z^0 exchange contributions [14, 15, 16, 17]. We point out that not only the branching ratio but also the decay distribution is sensitive to the MSSM parameters, giving us an extra handle to determine $m_{\tilde{l}}$, $\tan\beta$, M_i and μ, independent of the SUSY breaking mechanism.

The organization of this paper is as follows. In section 2, we discuss the MSSM parameter dependence of the lepton invariant mass distribution arising from $\tilde{\chi}_2^0$ decay. Near the region where interference between Z^0 exchange and $\tilde{l}$ exchange becomes important, the decay distribution is very sensitive to $m_{\tilde{l}}$. We point out that studying the whole distribution of the lepton invariant mass m_{ll} can be very important even for extracting the end point; events near the end point could be so few that one could misidentify it without this information. We also discuss the chiral structure of the amplitude, and show an interesting parameter dependence of the tau polarization in $\tilde{\chi}_2^0 \to \tau^+\tau^-\tilde{\chi}_1^0$ decays.

In section 3, we discuss effects of cuts on observed distributions. Though m_{ll} of lepton pairs from $\tilde{\chi}_2^0$ decay is independent of the $\tilde{\chi}_2^0$ boost, each lepton energy depends on the parent $\tilde{\chi}_2^0$ momentum. Therefore we expect two apparent sources of systematic error: (A) uncertainty of the lepton energy distribution in the $\tilde{\chi}_2^0$ rest frame, and (B) uncertainty of the parent $\tilde{\chi}_2^0$ momentum distribution. It would be helpful to reduce these two errors in order to maximize the physical information that can be extracted from the observed m_{ll} distribution. We argue that a measurement of the asymmetry of lepton energies would reduce the systematic errors from (A), while the lepton energy distribution near the end point of the m_{ll} distribution constrains (B). In section 4 we study if the m_{ll} distribution constrains $m_{\tilde{l}}$ and the parameters in the neutralino mass matrix. Section 5 is devoted to discussion and comments.

2 Lepton Invariant Mass Distribution

The branching ratio of the leptonic decay of the second lightest neutralino, $\tilde{\chi}_2^0 \to \tilde{\chi}_1^0 l^+ l^-$, is known to be very sensitive to the values of the underlying parameters. Three body decays of $\tilde{\chi}_2^0$ are dominant [14, 15, 16] as long as $\tilde{\chi}_2^0 \to \tilde{\chi}_1^0 Z^0$, $\tilde{\chi}_2^0 \to \tilde{l} l$ are not open. The dependence is enhanced by the negative interference between the decay amplitude from Z^0 exchange and that from slepton exchange. In the minimal supergravity model, the interference would be maximal when slepton masses are around 200 GeV [16].

In this section we show that the effect of the interference appears not only in the branching ratios, but also in the decay distributions, such as the distribution of the invariant mass m_{ll} of two the leptons.

We first show the differential partial width of the decay $\tilde{\chi}_A^0 \to \tilde{\chi}_B^0 \bar{f} f$ for a general light fermion f. We assume that the mass and Yukawa coupling of f, and left-right mixing of $\tilde{f}$ are negligible. The decay amplitude then consists of the Z^0 channel and the $\tilde{f}_{L,R}$ channel. The squared, spin averaged[2] amplitude $|\mathcal{M}|^2$ of the decay $\tilde{\chi}_A^0(p) \to \tilde{\chi}_B^0(\bar{p}) \bar{f}(\bar{q}) f(q)$ is written as follows:

$$\begin{aligned} |\mathcal{M}|^2 &= 2(A_{LL}^2 + A_{RR}^2)(1-y)(y - r_{\tilde{\chi}_B}^2) + 2(A_{LR}^2 + A_{RL}^2)(1-x)(x - r_{\tilde{\chi}_B}^2) \\ &\quad -4(A_{LL}A_{RL} + A_{RR}A_{LR}) r_{\tilde{\chi}_B} z, \end{aligned} \tag{1}$$

with

$$\begin{aligned} A_{LL} &= \frac{1}{2} g_Z^2 \frac{z_{BA}^{(\tilde{\chi}^0)} z_L^{(f)}}{z - r_Z^2} - \sum_X \frac{1}{2} g_2^2 \frac{a_{AX}^f a_{BX}^f}{y - r_{\tilde{f}_X}^2}, \\ A_{RL} &= -A_{LL}(y \leftrightarrow x), \\ \\ A_{LR} &= \frac{1}{2} g_Z^2 \frac{z_{BA}^{(\tilde{\chi}^0)} z_R^{(f)}}{z - r_Z^2} + \sum_X \frac{1}{2} g_2^2 \frac{b_{AX}^f b_{BX}^f}{x - r_{\tilde{f}_X}^2}, \\ A_{RR} &= -A_{LR}(y \leftrightarrow x), \end{aligned} \tag{2}$$

where $z_L^{(f)} = T_{3fL} - Q_f s_W^2$, $z_R^{(f)} = -Q_f s_W^2$, with $s_W^2 = \sin^2\theta_W$. The forms of the $\tilde{\chi}^0 \tilde{\chi}^0 Z^0$ couplings $z_{BA}^{(\tilde{\chi}^0)}$ and $\tilde{\chi}^0 f \tilde{f}$ couplings (a_{AX}^f, b_{AX}^f) are given in Appendix. (x, y, z) are phase space parameters of the decay defined as

$$x = (\bar{p} + q)^2 / m_{\tilde{\chi}_A^0}^2, \quad y = (\bar{p} + \bar{q})^2 / m_{\tilde{\chi}_A^0}^2, \quad z = (q + \bar{q})^2 / m_{\tilde{\chi}_A^0}^2, \tag{3}$$

[2]The polarization of $\tilde{\chi}_2^0$ might affect observed decay distributions. The effect depend on the process for $\tilde{\chi}_2^0$ production, and is not discussed in this paper.

with $x+y+z=1+m^2_{\tilde{\chi}^0_B}/m^2_{\tilde{\chi}^0_A}$. For convenience, we have introduced mass ratios $r_{\tilde{\chi}_B}$, r_Z, and $r_{\tilde{f}_X}$ as

$$r_{\tilde{\chi}_B}=m_{\tilde{\chi}^0_B}/m_{\tilde{\chi}^0_A},\ \ r_Z=m_Z/m_{\tilde{\chi}^0_A},\ \ r_{\tilde{f}_X}=m_{\tilde{f}_X}/m_{\tilde{\chi}^0_A}. \tag{4}$$

Note that (A_{LL}, A_{RL}) involve $(f_L, \bar{f}_R)$ while (A_{LR}, A_{RR}) involve $(f_R, \bar{f}_L)$. They do not interfere for $m_f=0$.

The partial decay width is given by

$$\frac{d\Gamma}{dx\,dy}(\tilde{\chi}^0_A\to\tilde{\chi}^0_B\bar{f}f)=\frac{N_C}{256\pi^3}m_{\tilde{\chi}^0_A}|\mathcal{M}|^2(x,y,z=1+r^2_{\tilde{\chi}_B}-x-y), \tag{5}$$

where $N_C=3(1)$ for $f=q(l)$. The range of $(x,\,y)$ is given by the conditions

$$\begin{aligned} z(xy-r^2_{\tilde{\chi}_B})&\geq 0,\\ r^2_{\tilde{\chi}_B}\leq x&\leq 1,\\ r^2_{\tilde{\chi}_B}\leq y&\leq 1,\\ x+y+z&=1+r^2_{\tilde{\chi}_B}. \end{aligned} \tag{6}$$

Now we consider the case of $\tilde{\chi}^0_2$ decay into $\tilde{\chi}^0_1 l^+ l^-$ under the assumption that all two body decays of $\tilde{\chi}^0_2$ are kinematically forbidden.[3]

In the phase space of the decay $\tilde{\chi}^0_2\to\tilde{\chi}^0_1 l^+ l^-$, the Z^0 exchange amplitude and $\tilde{l}$ exchange amplitude behave differently. When the Z^0 contribution dominates, distributions are enhanced in the region of large $m^2_{ll}=zm^2_{\tilde{\chi}^0_2}$. In contrast, when the $\tilde{l}$ exchange contribution dominates, distributions are enhanced in regions with large x and/or large y, therefore in small m_{ll} and large $|E^{\rm rest}_{l^-}-E^{\rm rest}_{l^+}|$ region. Here

$$E^{\rm rest}_{l^+}=(1-x)m_{\tilde{\chi}^0_2}/2,\ \ E^{\rm rest}_{l^-}=(1-y)m_{\tilde{\chi}^0_2}/2, \tag{7}$$

are lepton energies in the $\tilde{\chi}^0_2$ rest frame.

We consider the case where $2M_1\sim M_2\ll|\mu|$, a typical case in the minimal supergravity model. In this case, $\tilde{\chi}^0_2$ is Wino-like and $\tilde{\chi}^0_1$ is Bino-like. An interesting property in this case is that the Z^0 and $\tilde{l}$ amplitudes could be of comparable size in some region of phase space. Furthermore, their interference is generally destructive for leptonic decays. These effects cause complicated situations, which we discuss below.

We show numerical results for the m_{ll} distribution. For illustration, we use two sets of parameters for the neutralino sector, (A) and (B), shown in Table 1. These values are fixed to give the same masses for three inos, ($m_{\tilde{\chi}^0_1}$,

[3]In some region of parameter space, we may study the three body decays of $\tilde{\chi}^0_2$ even if two body decays are open [18]. Such a study is beyond the scope of this paper.

set	M_1	M_2	μ	$\tan\beta$
(A)	70	140	–300	4
(B)	77.6	165	286	4

Table 1: Parameter sets for neutralinos. All entries with mass units are in GeV.

$m_{\tilde{\chi}_2^0}$, $m_{\tilde{\chi}_2^+}$) = (71.4, 140.1, 320.6) GeV. For calculating the branching ratios, we take generation-independent slepton masses and a universal soft SUSY breaking squark mass $m_{\tilde{Q}} = 500$ GeV.

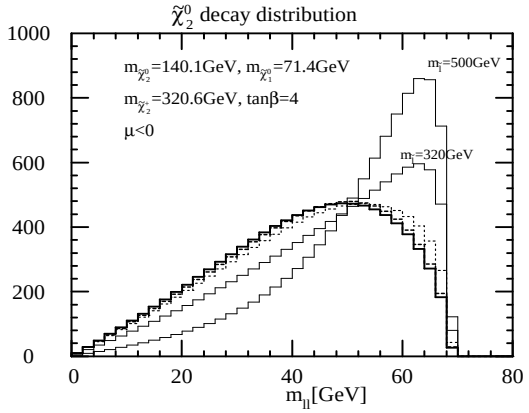

Figure 1: Invariant mass distribution of the lepton pairs from $\tilde{\chi}_2^0$ three body decay. The neutralino parameters are taken as set (A) (see Table 1), and universal slepton masses $m_{\tilde{l}} = m_{\tilde{l}_L} = m_{\tilde{l}_R}$ are 170 GeV (thick solid), 220 GeV (dashed), 270 GeV (dotted), 320 GeV, and 500 GeV. For $m_{\tilde{Q}} = 500$ GeV, $Br(\tilde{\chi}_2^0 \to e^+e^-\tilde{\chi}_1^0)$ =11%, 9.5%, 4.1%, 2.1%, 1.9%, respectively. The total number of events of each curve is 10^4.

In Fig. 1, we show the m_{ll} distribution of the decay $\tilde{\chi}_2^0 \to l^+l^-\tilde{\chi}_1^0$ for parameter set (A) and varying $m_{\tilde{l}}$ from 170 GeV to 500 GeV. [4]

Because $m_{\tilde{\chi}_2^0}$ and $m_{\tilde{\chi}_1^0}$ are fixed, the end points of the distributions $m_{ll}^{\max} =$ 68.7 GeV are same for each curve, while the shape of the distribution changes drastically with slepton mass. For a slepton mass of 170 GeV (thick solid line), the decay proceeds dominantly through slepton exchanges, therefore

[4]Heavy sleptons and Bino-like $\tilde{\chi}_1^0$ is cosmologically disfavored because it leads to a large relic mass density [19]. However, this constraint can easily be evaded if $\tilde{\chi}_1^0$ can decay, or if there is late time entropy production.

the m_{ll} distribution is suppressed near $m_{ll}^{\max}$. On the other hand, once slepton exchange is suppressed by its mass, Z^0 exchange dominates and the distribution peaks sharply near $m_{ll}^{\max}$. Notice that the leptonic branching ratio decreases as $m_{\tilde{l}}$ increases, but remains larger than $\sim$2% for the values of $m_{\tilde{l}}$ taken in the figure.

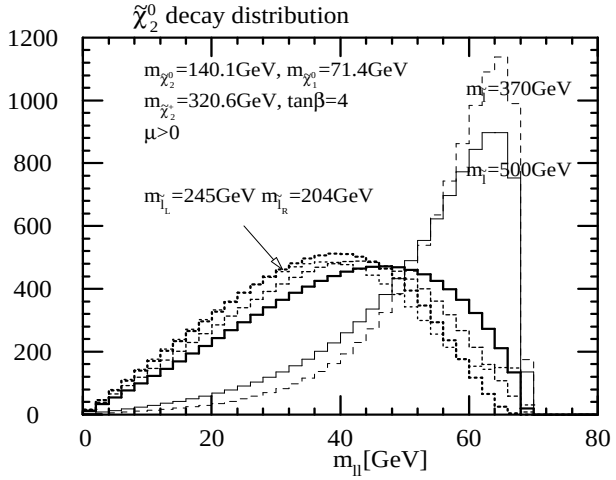

Figure 2: m_{ll} distribution for parameter set (B) ($\mu > 0$). $m_{\tilde{l}_L} = m_{\tilde{l}_R}$ are 170 GeV (thick solid), 220 GeV (dashed), 250 GeV (dotted), 370 GeV, and 500 GeV. The branching ratio $Br(\tilde{\chi}_2^0 \to e^+e^-\tilde{\chi}_1^0)$ for $m_{\tilde{Q}} = 500$ GeV is 6.6%, 2.9%, 0.9%, 1%, 1.8%, respectively, The thick dashed line is an example with complete cancellation of the amplitude near the upper end point. The branching ratio to $e^+e^-\tilde{\chi}_1^0$ is 1.8% for this case. The total number of the events is 10^4 for each curve.

In Fig. 2, we show an example for $\mu > 0$, parameter set (B). The dependence on the slepton mass is different from the previous case. As $m_{\tilde{l}}$ increases from 170 GeV, m_{ll} distribution becomes softer. For $m_{\tilde{l}} > 250$ GeV, a second peak appears due to strong cancellation of Z^0 exchange and slepton exchange contributions for a certain value of m_{ll}. At the same time, the branching ratio reaches its minimum at $m_{\tilde{l}} \sim 300$ GeV, much less than 1%. For $m_{\tilde{l}} \gg 370$ GeV, it increases again above 1%.

Notably, one can find slepton masses where a complete cancellation occurs very close to the end point $m_{ll}^{\max}$ of the m_{ll} distribution. The thick dashed line shows distribution for $m_{\tilde{l}_L} = 245$ GeV and $m_{\tilde{l}_R} = 204$ GeV. Events near the end point ($m_{ll}^{\max} - m_{ll} < 4$ GeV) becomes too few, and it is very hard to observe the real end point for this case.

The lepton invariant mass distribution is an important tool for studying

supersymmetric models at hadron colliders. In [8], a case study is done in a scenario where decays $\tilde{g} \to b\tilde{b}$ and $\tilde{b} \to b\tilde{\chi}_2^0$ have substantial branching ratios. $\tilde{\chi}_2^0$ production is enhanced by the large gluino production cross section, and the S/N ratio could be improved substantially by requiring three or four bottom jets in the final states. For $Br(\tilde{\chi}_2^0 \to e^+e^-\tilde{\chi}_1^0) \sim 16$ %, S/N goes well above 10. Even if gluino decay into $\tilde{b}b$ is closed, the lepton invariant mass distribution can be measured (case 4 of [8]). In this case, one can subtract most backgrounds using lepton pair samples with opposite charge and different flavors.

The most important aspect of the lepton invariant mass distribution in these studies is the determination of the end point, which is expected to coincide with $m_{\tilde{\chi}_2^0} - m_{\tilde{\chi}_1^0}$. Furthermore, choosing events near the end point helps one to relate the velocity of the two lepton system β_{ll} to that of the neutralinos $\beta_{\tilde{\chi}_2^0}$ and $\beta_{\tilde{\chi}_1^0}$, so that one can reconstruct the cascade decay chain. Errors on the mass difference of $2\% \sim 0.1\%$ are claimed depending on statistics [8].

The slepton mass dependence of $\tilde{\chi}_2^0$ decay distributions suggests that not only the end point of the distributions but also the distributions themselves contain information about the underlying parameters such as $m_{\tilde{l}}$. The negative side of this is that the fitted end point may depend on the assumed values of these parameters, introducing additional systematic errors in the fit. For some extreme case shown in Fig. 2, the observed end point of the lepton invariant mass distribution does *not* coincide with $m_{\tilde{\chi}_2^0} - m_{\tilde{\chi}_1^0}$. Note that realistic simulations including the parameter dependence of the decay distribution are not available for hadron colliders so far. In the commonly used Monte Carlo (MC) simulators ISAJET [20] and SPYTHIA [21], the three body decay distribution of sparticles is approximated by the phase space distribution, while branching ratios are calculated by full expressions.[5] See section 3 (especially Fig. 4) for comparison between real m_{ll} distribution and the distribution in phase space approximation.

For the case shown in Figs. 1 and 2, $Br(\tilde{\chi}_2^0 \to \tilde{\chi}_1^0 l^+ l^-)$ is not always large. It has not been yet studied systematically if it is possible to measure the lepton decay distribution at future hadron and e^+e^- colliders when $Br(\tilde{\chi}_2^0 \to \tilde{\chi}_1^0 l^+ l^-)$ is small. Given small Standard Model backgrounds, a study of distribution may be possible when $Br(\tilde{\chi}_2^0 \to e^+e^-\tilde{\chi}_1^0) \gtrsim 2\%$ for not too heavy gluino. At future lepton colliders, it is very easy to get a clean signal. However, the production cross section is rather small for heavy sleptons.

[5] The most recent ISAJET release (ISAJET 7.43) allows to simulate the effect of exact matrix elements for all three body decay distributions. In the codes used for CERN LEP [22] and JLC1 [23] studies, the effect is already included.

At e^+e^- collider with large luminosity ($\int \mathcal{L} > 500$ fb^{-1}/yr) [24], the region with $\sigma(e^+e^- \to \tilde{\chi}_2^0\tilde{\chi}_2^0) > 20$ fb may be studied with samples containing more than 1000 events, even if $Br(\tilde{\chi}_2^0 \to e^+e^-\tilde{\chi}_1^0) \sim$ a few %.

In Figs. 1 and 2, we found that the decay distributions depend on sign(μ). The difference comes from neutralino mixings. For the parameter set (A), $\tilde{\chi}_2^0$ has small Bino component; $(N_{21}, N_{22}, N_{23}, N_{24}) = (7.25\times10^{-4}, 0.957, -0.281, -6.90\times10^{-2})$ where $\tilde{\chi}_i^0 = N_{i1}\tilde{B} + N_{i2}\tilde{W}^3 + N_{i3}\tilde{H}_1^0 + N_{i4}\tilde{H}_2^0$. It does not couple to $\tilde{l}_R$ effectively [see Eq. (A4)], therefore decay into l_R proceeds dominantly through Z^0 exchange. In Fig. 3(a) we show the m_{ll} distribution for $l^+l_R^-$(dotted lines) and $l^+l_L^-$(dashed lines) for $m_{\tilde{l}} = 220$ GeV(thick lines) and 270 GeV(thin lines). When $m_{\tilde{l}}$ increases from 220 GeV to 270 GeV, $|\mathcal{M}_L|^2 = |\mathcal{M}(\tilde{\chi}_1^0 l^+ l_L^-)|^2$ is suppressed near $m_{ll}^{\max}$ and also becomes smaller due to interference. The relative importance of $|\mathcal{M}_R|$ increases, leading to a total distribution that is more strongly peaked near $m_{ll}^{\max}$. On the other hand, for parameter set (B) ($\mu > 0$), $\tilde{\chi}_2^0$ still has substantial Bino component; $(N_{21}, N_{22}, N_{23}, N_{24}) = (0.196, 0.902, -0.322, 0.212)$. As $m_{\tilde{l}}$ increases, negative interference appears near $m_{ll} = m_{ll}^{\max}$ for both $|\mathcal{M}_L|$ and $|\mathcal{M}_R|$, leading to a suppression of the m_{ll} distribution near $m_{ll}^{\max}$.

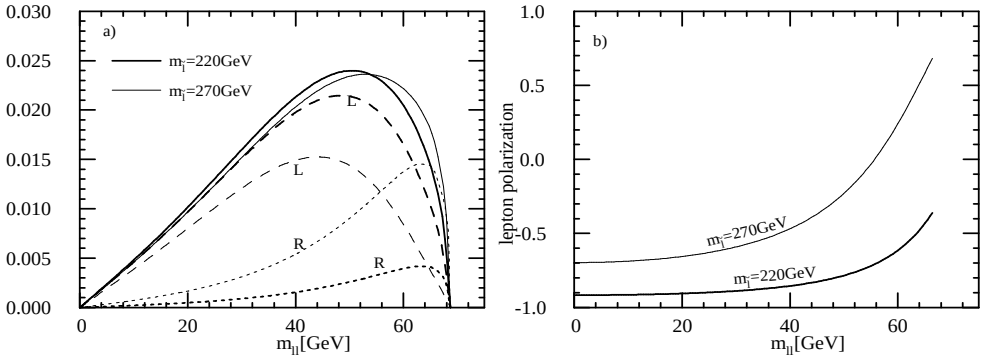

Figure 3: (a) m_{ll} distribution from $\tilde{\chi}_2^0 \to \tilde{\chi}_1^0 l^+ l^-$ decays for $m_{\tilde{l}} = 220$ GeV and $m_{\tilde{l}} = 270$ GeV and parameter set (A). The dashed lines show $l^+l_L^-$ distribution, the dotted lines for $l^+l_R^-$ distribution, the solid lines for total. The curves are normalized so that the total widths are the same. (b) Polarization of lepton l^- [$\equiv (N_R - N_L)/(N_R + N_L)$] arising from $\tilde{\chi}_2^0$ decay. Average polarization is $P_{ave} = -0.839$ for $m_{\tilde{l}} = 220$ GeV and -0.428 for $m_{\tilde{l}} = 270$ GeV.

In Fig. 3(a), negative interference reduces the amplitude near $m_{ll}^{\max}$ for l_L^-, while the amplitude for l_R^- is increased. This causes a strong m_{ll} dependence of the lepton polarization P_l. In Fig. 3(b), we plot this polarization as a func-

tion of m_{ll} for different slepton masses. They differ dramatically near $m_{ll}^{\max}$. In neutralino decays into $\tau^+\tau^-\tilde{\chi}_1^0$, P_τ may be observed through the decay distributions of the τ leptons. In $\tau^\pm \to \rho^\pm \to \pi^\pm\pi^0$, $a_1 \to \pi^\pm\pi^0\pi^0$ decays, the $E_{\pi^\pm}/E_{jet}$ distribution depends on the parent τ polarization drastically [25]. Experimentally, the fine momentum resolution [1, 7] of the detector could be used to identify these tau decay products [5] at future e^+e^- colliders. At hadron colliders, the momentum of charged tracks and the energy deposited in the electromagnetic calorimeter would give the same information. Implications of τ polarization measurements in analyses of new physics have been discussed for charged Higgs bosons produced at the upgraded Tevatron and LHC colliders [26], and for $\tilde{\tau}$ at e^+e^- colliders [27, 5].

Due to the missing tau neutrinos, one would not be able to measure the invariant mass of two tau leptons. Nevertheless the P_τ dependence on the invariant mass of the two τ jets might be seen in future collider experiments. Note that in $\tau \to \rho$ or a_1 decays, the final vector meson carries a substantial part of the parent τ momentum, therefore the smearing of the distribution is less severe than for decays into $\pi^\pm$, μ, and e.

Several comments are in order. In Eq. (1), we have neglected the Yukawa couplings of leptons and slepton left right mixing. For $\tilde{\tau}$, these effects could be very important if $\tan\beta$ is large. Notice that their leading contribution flips the chirality of the τ lepton [27]. For three body decays, studying the correlation of two tau decay distributions would reveal the helicity flipping and conserving contributions separately.

In most numerical calculations in this paper, we assume universality of slepton masses. However, in supersymmetric model, staus could be lighter than the other sleptons for various reasons. The running of stau soft SUSY breaking masses from the Planck scale [28] and stau left-right mixing [29] could enhance decays into $\tau\tilde{\tau}$ or $\tau^+\tau^-\tilde{\chi}_1^0$. Experimental consequences of such scenarios have recently been widely discussed [30, 31]. Also models with lighter third generation sparticles have been constructed to naturally avoid the flavor changing neutral current problem [13]. The two body decay branching ratio into $\tau\tilde{\tau}$ or the three body decay branching ratio into $\tau\tau\tilde{\chi}_1^0$ and the decay distribution might be different from those for leptons in the first two generations. The study of the $\tilde{\chi}_2^0 \to \tau^+\tau^-\tilde{\chi}_1^0$ decay in addition to the other leptonic modes could be an important handle to identify such models.

3 Correcting Acceptance Errors

In collider experiments, we need cuts to reduce backgrounds, and they substantially change distributions we are interested in. This effect can be corrected by Monte Carlo simulations once model parameters are fixed. But it is still worthwhile to investigate how the distributions are modified by the cuts, and if this effect can be estimated in a model-independent way.

Let us consider $\tilde{\chi}_2^0$ decays at the LHC, where $\tilde{\chi}_2^0$ comes from the cascade decay of heavier squarks and gluinos:

$$\begin{aligned} \tilde{q} &\rightarrow \begin{cases} \tilde{g}q \text{ (if } m_{\tilde{q}} > m_{\tilde{g}}), \\ q\tilde{\chi}_2^0, \end{cases} \\ \tilde{g} &\rightarrow \begin{cases} q\bar{q}\tilde{\chi}_2^0, \\ q\tilde{q} \text{ (if } m_{\tilde{q}} < m_{\tilde{g}}), \end{cases} \end{aligned} \tag{8}$$

and $\tilde{\chi}_2^0$ may decay further into $l^+l^-\tilde{\chi}_1^0$. These decay processes have been shown to have small backgrounds. In [8], $\tilde{g}$ decay into $b\tilde{b}$ followed by $\tilde{b} \rightarrow b\tilde{\chi}_2^0$, and $\tilde{g}$ decay into $qq\tilde{\chi}_2^0$ were studied. After lepton transverse momentum cuts, cuts on total transverse energy E_T and total missing transverse energy $\not{E}_T$, b tagging (for the former), and subtraction of backgrounds estimated from the opposite charge – different flavor lepton sample, the m_{ll} distribution from $\tilde{\chi}_2^0$ decays can be measured over a wide region of m_{ll}.

The observed distributions are modified by the cuts, and they depend on the decay processes through which $\tilde{\chi}_2^0$ is produced. One might worry that those cuts are strongly correlated with m_{ll}, i.e., particular regions of m_{ll} have large (small) acceptance, therefore the whole distribution may become quite different from the original one. Indeed, the cuts on lepton energy should affect the m_{ll} distribution directly. On the other hand, cuts on the total E_T and $\not{E}_T$ should be less correlated with the momenta of the leptons. In the following, we therefore discuss the effect of cuts on lepton energies on the lepton invariant mass distribution.

In Ref. [8], a lepton transverse momentum cut, $p_T^l > 10$ GeV $\sim$15 GeV, is applied to all leptons. The m_{ll} distribution after this cut should depend on the E_l distributions of $\tilde{\chi}_2^0$ decays in the $\tilde{\chi}_2^0$ rest frame, and also on the $\tilde{\chi}_2^0$ momentum distribution through the boost of leptons. In Fig. 4, we plot the m_{ll} distribution for our standard parameter set (A) and $m_{\tilde{l}} = 250$ GeV, requiring that the lepton energy E_l in the $\tilde{\chi}_2^0$ rest frame is larger than 0 (thick solid), 10 GeV (thick dashed), 15 GeV (thick dotted), respectively. We also plot the corresponding distributions in phase space approximation.

Figure 4 reproduces the quantitative effects of p_T^l cut. Because of the lepton p_T cuts, leptons with $E_l < p_T^{l\text{cut}}$ have no chance of being accepted

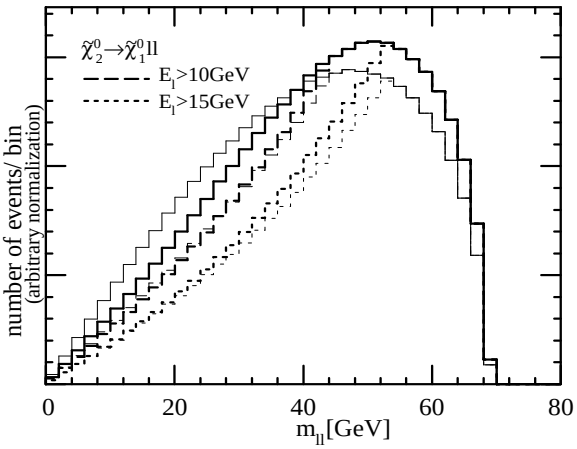

Figure 4: Invariant mass distributions of the lepton pairs from $\tilde{\chi}_2^0$ decay for the parameter set (A) and $m_{\tilde{l}} = 250$ GeV (thick lines). $E_l > 0$ (solid line), 10 GeV (dashed), and 15 GeV (dotted) is required. We also show the distributions in phase space approximation by thin lines.

unless the parent neutralino has enough transverse momentum. Therefore the dashed and dotted lines show quantitative nature of the m_{ll} distribution after the p_T^l cut when the momentum of the parent neutralino is negligible. Typically, events with large m_{ll} have a better chance of being accepted. We can see that both of the leptons have energy larger than 15 GeV if $m_{ll} > 54$ GeV. $E_l^{\rm rest} \sim 35$ GeV in the region close to $m_{ll}^{\rm max}$. Unless leptons go in the beam direction, they would be accepted. Although the actual distribution after the p_T^l cut would depend on the p_T distribution of $\tilde{\chi}_2^0$, it is still qualitatively true that events with small m_{ll} would be more affected by the cuts. Note that, whenever a large cancellation of the amplitude occurs at the m_{ll} end point, the m_{ll} distribution near the end point also differs substantially from those without cancellation. The acceptance near the end point should be large and should depend on m_{ll} only weakly, so that we could distinguish a "fake" end point from the kinematical one through the study of the distribution.

In Fig. 4, the m_{ll} distribution is softer in the phase space approximation. However, when $E_l^{\rm rest} > 10$ GeV is required, the number of events with smaller m_{ll} is reduced significantly compared with that for parameter set (A). The qualitative difference between the two curves becomes less significant after $E_l^{\rm rest} > 10$ GeV is required.

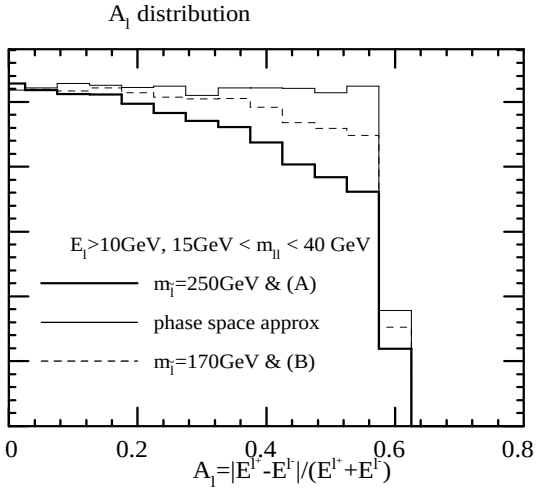

Figure 5: $A_l = |E_{l^+}^{\rm rest} - E_{l^-}^{\rm rest}|/\ (E_{l^+}^{\rm rest} + E_{l^-}^{\rm rest})$ distribution of the lepton pair from $\tilde{\chi}_2^0$ decays with 15 GeV$< m_{ll} <$ 40 GeV and $E_l > 10$ GeV. The thick solid line is for $m_{\tilde{l}} = 250$ GeV and the parameter set (A), the dashed line for $m_{\tilde{l}} = 170$ GeV and the parameter set (B), and the solid line for phase space approximation. Curves are normalized to coincide at $A_l = 0$.

The difference of the acceptance in smaller m_{ll} region can be seen when we plot lepton energy difference. In Fig. 5 we plot $A_l = |E_{l^+} - E_{l^-}|/(E_{l^+} + E_{l^-})$ in the rest frame of $\tilde{\chi}_2^0$ requiring $E_l > 10$ GeV and[6] 15 GeV $< m_{ll} <$ 40 GeV. The distribution reaches its maximum at $A_l = 0$ for the parameter set (A) with $m_{\tilde{l}} = 250$ GeV (thick line), while for phase space approximation (solid) the A_l distributions are roughly flat. This is because the amplitude near $E_l^{\rm rest} = 0$ is suppressed, and agrees with the quantitative difference of the acceptance in small m_{ll} region found in Fig. 4. The acceptance should also depend on underlying MSSM parameters. We show the distribution for the parameter set (B) and $m_{\tilde{l}} = 170$ GeV, which has similar m_{ll} distribution to $\mu < 0$ case. Due to the small slepton masses, the amplitude is enhanced in smaller E_l region, therefore the A_l distribution is more flat than for the $m_{\tilde{l}} = 250$ GeV case. This suggests that A_l and acceptance may depend on slepton masses when $\tilde{\chi}_2^0 \to \tilde{l}l$ is about to open.

It might be possible to determine the lepton energy asymmetry directly. In Ref. [18], the correlation between the A_l and A_l^T distributions is studied

[6]Here we restrict m_{ll} from 15 GeV to 40 GeV. We may have a background of $\gamma^* \to l^+l^-$ in small m_{ll} region. For m_{ll} near the end point, leptons tend to have equal energy, and the contribution to A_l is insignificant.

for the $\tilde{\chi}_2^0$ decay into $\tilde{l}_R l$. Here $A_l^T \equiv |p_T^{l^+} - p_T^{l^-}|/(p_T^{l^+} + p_T^{l^-})$, where $p_T^{l^+}$ and $p_T^{l^-}$ are transverse momenta of the two identified leptons. In the two body decay, A_l in the $\tilde{\chi}_2^0$ rest frame is restricted to a rather small region. Although $\tilde{\chi}_2^0$ originates from gluino or squark decays and should have some transverse momentum for the case studied in that paper, the A_l^T distribution is still peaked where the A_l distribution is located. This shows that A_l^T reflects the decay distribution in the $\tilde{\chi}_2^0$ rest frame.

The acceptance would also depend on the $\tilde{\chi}_2^0$ momentum distribution. If $\tilde{\chi}_2^0$ has large transverse momentum, events with smaller $E_l^{\rm rest}$ would have a better chance of being accepted. Notice that if $E_l^{\rm rest} < p_T^{l\rm cut}$, this is the only possibility for the events being accepted; certainly the $\tilde{\chi}_2^0$ transverse momentum distribution must be determined somehow to make a reliable estimate of the acceptance.

Naturally, an average $p_{T\tilde{\chi}_2^0}$ of the order of $m_{\tilde{g}(\tilde{q})}$ is expected when the $\tilde{\chi}_2^0$ comes from $\tilde{q}$ or $\tilde{g}$ decay. The tree level kinematical distribution is determined by parent and daughter masses if the $\tilde{\chi}_2^0$ originated from a two body decay. Existing MC simulations describe the two body decay distributions correctly. For the three body decay, the distributions are different from those in phase space approximation. However, there would be no significant parameter dependence because only squark exchange contributes to the decay modes in Eq. (8). If we have direct information on those masses, it may be rather easy to estimate the transverse momentum distribution[7] of $\tilde{\chi}_2^0$.

The $\tilde{\chi}_2^0$ distribution can be measured directly if there is substantial statistics near the m_{ll} end point. At the end point, the total momentum of the lepton pair is zero in the $\tilde{\chi}_2^0$ rest frame, and we could reconstruct the velocity of $\tilde{\chi}_2^0$, $\vec{\beta}_{\tilde{\chi}_2^0}$, from the momentum of the lepton pair [7, 8]. This $\tilde{\chi}_2^0$ distribution may be convoluted with the m_{ll} distribution and the A_l distribution in the $\tilde{\chi}_2^0$ rest frame to obtain the corresponding distributions in the laboratory frame. Even though the observed decay distributions are sensitive to the $\vec{p}_{\tilde{\chi}_2^0}$ spectrum, they might thus be corrected by measuring the $\vec{\beta}_{\tilde{\chi}_2^0}$ distribution using events with m_{ll} near its end point.

So far we have only discussed the invariant mass distribution of lepton pairs from $\tilde{\chi}_2^0$ decays, which is known to be important for SUSY studies at the LHC. In contrast, for the Tevatron upgrade, the trilepton mode is more important to discover supersymmetry [32, 30]. This signal comes from the coproduction of $\tilde{\chi}_2^0\tilde{\chi}_1^\pm$ and their decays into leptons. For this particular mode, the energy distribution of leptons from chargino decay must be considered

[7]However, the transverse momentum of gluino receives (SUSY) QCD corrections. Correct estimation of the distribution would be very important.

in addition to the neutralino decay distributions.

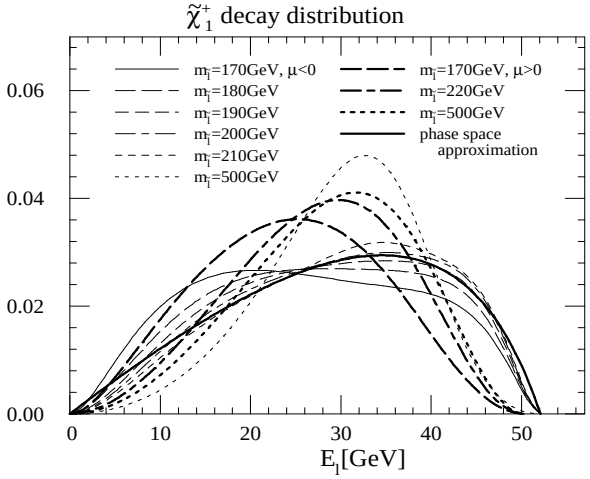

Figure 6: Energy distribution of the charged lepton from $\tilde{\chi}_1^+ \to \tilde{\chi}_1^0 l^+ \nu$ decay in the $\tilde{\chi}_1^+$ rest frame. We take parameter set (A) ($\mu < 0$) and (B) ($\mu > 0$) and vary $m_{\tilde{l}}$ as indicated in the figure. The thick solid line shows the distribution in the phase space approximation. The leptonic branching ratio of $\tilde{\chi}_1^+$ is above 8% for the parameters used in the figure.

In Fig. 6, we show the lepton energy distribution of chargino $\tilde{\chi}_1^+$ in the chargino rest frame for the parameter sets (A) and (B). The amplitude of χ_1^+ decay is easily obtained by replacing relevant masses and couplings in Eq. (1). The parameter dependence is not very strong if the slepton mass is much above 200 GeV, but if it is close to $\tilde{\chi}_1^+$, the lepton energy distribution sensitively depends on the slepton mass. The branching ratio to the lepton is also larger in this region making the trilepton mode more promising. For parameter set (A), the distribution is almost flat in E_l for $m_{\tilde{l}} = 170$ GeV. Such a dependence of the energy distribution in the $\tilde{\chi}_1^\pm$ rest frame on MSSM parameters will affect the observed distribution of leptons in the lab frame. Notice that we must also pay attention to the effect of other cuts, e.g., on the total E_T or $\not{E}_T$. For example, for $\tilde{\chi}_2^0 \tilde{\chi}_1^\pm$ co-production, the two $\tilde{\chi}$ have balanced transverse momentum unlike in the case where $\tilde{\chi}_2^0$ comes from $\tilde{g}$ decay. The two $\tilde{\chi}_1^0$ from $\tilde{\chi}_2^0$ and $\tilde{\chi}_1^\pm$ decays tend to be back to back to each other. This makes the total $\not{E}_T$ smaller, especially when the lepton energies are large. The correlation between various cuts must be studied very carefully.

In this section, we have only discussed the effect of lepton energy cuts on the observed m_{ll} distribution, and its dependence on unknown MSSM

parameters. It is possible that other cuts like lepton isolation cuts, $\not{E}_T$ cuts, and total E_T cuts correlate with each other in a complicated manner to introduce additional uncertainties. This may be corrected quite easily by existing MC simulations. The aim of this section has been to point out an obvious source of uncertainty that has not been taken into account in current MC simulations, and to propose several observables that might constrain this uncertainty directly.

4 Sensitivity to the Underlying Parameters

In this section, we discuss if it is possible to extract the values of underlying MSSM parameters by measuring the m_{ll} distribution. As we have already seen the distribution depends strongly on $m_{\tilde{l}}$, and also on the $\tilde{\chi}_2^0\tilde{\chi}_1^0 Z$ and $\tilde{\chi}_2^0 l\tilde{l}$ couplings. The latter is determined by the Higgsino components of $\tilde{\chi}_2^0$ and $\tilde{\chi}_1^0$. Because we take these neutralinos to be gaugino-like, their Higgsino components come from gaugino-Higgsino mixing. It depends on $\tan\beta$ and the Higgsino mass parameter μ, and $|\mu|$ is roughly equal to $m_{\tilde{\chi}_3^0}$, $m_{\tilde{\chi}_4^0}$ or $m_{\tilde{\chi}_2^+}$. Therefore the m_{ll} distribution gives at least one constraint on μ, $\tan\beta$ and $m_{\tilde{l}}$ in addition to the well known constraint on $m_{\tilde{\chi}_2^0} - m_{\tilde{\chi}_1^0}$.

Because there is no MC simulation including the parameter dependence of three body decay distributions, we estimate the sensitivity to $\tan\beta$ and $m_{\tilde{l}}$ under the following *working* assumptions:

1. Backgrounds can be subtracted, or are negligible, and do not cause additional systematic errors.

2. The dependence of the acceptance on m_{ll} can be corrected.

Under these assumptions, we define the sensitivity function $\mathcal{S}$ as follows:

$$\begin{aligned}&\mathcal{S}\left(M_1, M_2, \mu, \tan\beta, m_{\tilde{l}_{L,R}}|_{\rm fit}; M_1, M_2, \mu, \tan\beta, m_{\tilde{l}_{L,R}}|_{\rm input}\right)\\ &= \sqrt{\sum_i \left(n_i^{\rm fit} - n_i^{\rm input}\right)^2 / n_i^{\rm input}}\,. \end{aligned} \tag{9}$$

Here $n_i^{\rm fit}$ ($n_i^{\rm input}$) is the number of events in the i-th bin of the m_{ll} distribution for the MSSM parameters $(M_1, M_2, \mu, \tan\beta, m_{\tilde{l}_{L,R}})|_{\rm fit(input)}$. We normalize $\sum_i n_i^{\rm fit} = \sum_i n_i^{\rm input}$ to some number N. Then $\mathcal{S}$ gives the deviation of the input distribution $n_i^{\rm input}$ from the distribution for the fit ($n_i^{\rm fit}$) in units of standard deviations. We take[8] $N = 2500$ and an m_{ll} bin size of 2 GeV.

[8] The available number of lepton pairs from $\tilde{g}$ decay ranges from 10^6 to 1000 for 10

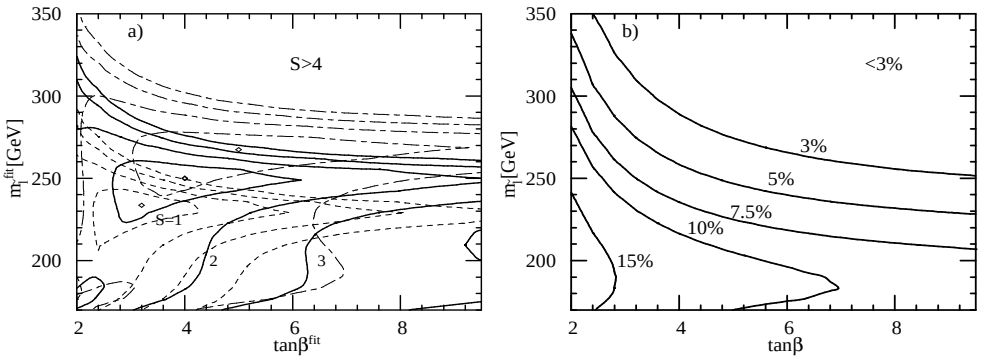

Figure 7: (a) Contours of constant sensitivity function $\mathcal{S} = 1, 2, 3, 4$ in the $(\tan\beta^{\rm fit},\, m_{\tilde{l}}^{\rm fit})$ plane. See text for the definition of $\mathcal{S}$. Input parameters are set (A) with $m_{\tilde{l}} = 250$ GeV. For solid lines, we fix $m_{\tilde{\chi}_2^0}$, $m_{\tilde{\chi}_1^0}$ and $m_{\tilde{\chi}_2^+}$ equal to those for parameter set (A) by varying $M_1^{\rm fit}$, $M_2^{\rm fit}$ and $\mu^{\rm fit}$, while $\tan\beta^{\rm fit}$ and $m_{\tilde{l}}^{\rm fit}$ are varied to see the sensitivity of the $\tilde{\chi}_2^0$ decay distribution to these parameters. For the dot-dashed (dashed) lines, $m_{\tilde{\chi}_2^+}^{\rm fit} = m_{\tilde{\chi}_2^+}^{\rm input} + (-)30$ GeV have been taken. Diamonds correspond to the best fit points of each fit. (b) Contours of constant $Br(\tilde{\chi}_2^0 \to \tilde{\chi}_1^0 l^+ l^-)$ in the $\tan\beta$ and $m_{\tilde{l}}$ plane. The masses of $\tilde{\chi}_2^0$, $\tilde{\chi}_1^0$, and $\tilde{\chi}_2^+$ are set to equal to those for parameter set (A).

In Fig. 7(a), we show contours of constant $\mathcal{S} = 1, 2, 3, 4$ (corresponding to 1σ, 2σ, 3σ, 4σ) in the $(\tan\beta^{\rm fit},\, m_{\tilde{l}}^{\rm fit})$ plane. For the solid lines, we take parameter set (A) and $m_{\tilde{l}} = 250$ GeV as input parameters, while for fitting parameters we vary $\tan\beta$ and $m_{\tilde{l}_L} = m_{\tilde{l}_R}$, fixing $(M_1^{\rm fit},\, M_2^{\rm fit},\, \mu^{\rm fit})$ to reproduce the input values of $(m_{\tilde{\chi}_1^0},\, m_{\tilde{\chi}_2^0},\, m_{\tilde{\chi}_2^+})$.[9] The resulting contours (solid lines) correspond to the sensitivity of the m_{ll} distribution to $m_{\tilde{l}}$ and $\tan\beta$ when the three ino masses are known.

In the figure, a strong upper bound on the slepton masses emerges, while the lower bound is weak. Notice that there is another minimum near $\tan\beta \sim 2$ and $m_{\tilde{l}} = 170$ GeV. By looking at the A_l^T distribution, the two different minima may be distinguished. In that case a stronger lower bound would be obtained. On the other hand, $m_{\tilde{l}} < 260$ (270) GeV is obtained if $\mathcal{S} < 1$ (2) is required. This can be understood as a result of the large change of the

fb^{-1} in the LHC study [8] for a grand unified theory (GUT) scale gaugino mass parameter $M = 100$ GeV. At a high luminosity e^+e^- collider, $\mathcal{O}(1000)$ lepton pairs could be produced. Our choice $N = 2500$ should thus not be too unrealistic.

[9] In our fit, we fix the ino masses, therefore we implicitly assume that the "fake end point" problem discussed in section 2 can be resolved when the whole distributions are taken into account.

distribution between $m_{\tilde{l}} = 270$ GeV and $m_{\tilde{l}} = 500$ GeV found in Fig. 1. The m_{ll} distribution also constrains $\tan\beta$ mildly. The constraint is not very strong due to our choice of parameters $|\mu| \gg M_2$; gaugino-Higgsino mixing is suppressed in this case.

We computed these contours by fixing the three ino masses. This may not be a realistic assumption, because $\tilde{\chi}_2^{\pm}$ might not be observed at the LHC. If we perform the fitting with varied $m^{\rm fit}_{\tilde{\chi}_2^+}$, we can find almost the same m_{ll} distribution for different sets of parameters. In Fig. 7, the dashed (dot-dashed) lines correspond to constant $\mathcal{S}$ contours when $m^{\rm fit}_{\tilde{\chi}_2^+} = m^{\rm input}_{\tilde{\chi}_2^+} - 30$ GeV ($m^{\rm fit}_{\tilde{\chi}_2^+} = m^{\rm input}_{\tilde{\chi}_2^+} + 30$ GeV) is required for the fitting. The best fit points are $\tan\beta = 3.2$ and $m_{\tilde{l}} = 233.6$ GeV for $m^{\rm fit}_{\tilde{\chi}_2^+} = m^{\rm input}_{\tilde{\chi}_2^+} - 30$ GeV, and $\tan\beta = 5$ and $m_{\tilde{l}} = 267$ GeV for $m^{\rm fit}_{\tilde{\chi}_2^+} = m^{\rm input}_{\tilde{\chi}_2^+} + 30$ GeV. The best fit point therefore moves from smaller $\tan\beta$ and $m_{\tilde{l}}$ to larger ones as $m^{\rm fit}_{\tilde{\chi}_2^+}$ is increased. Other distributions such as p_T^l and A_l^T might differ at different best fit points; however, we do not go into the details of these distributions.

At each best fit point with different $m^{\rm fit}_{\tilde{\chi}_2^+}$, $\mathcal{S} \sim 0$. Therefore the dashed or dot-dashed contours are very similar to the contours of constant $\mathcal{S}$ where the parameters for the best fit point are taken as the inputs. It can be seen that as $m_{\tilde{\chi}_2^+}$ is decreased, the constraint on $\tan\beta$ becomes stronger, because Higgsino-gaugino mixing becomes more important. On the other hand, when $m^{\rm fit}_{\tilde{\chi}_2^+}$ is increased, the constraint on $\tan\beta$ tends to disappear.

The constraint from the m_{ll} distribution is independent of that from the decay branching ratio. In Fig. 7(b), we show the contours of constant $Br(\tilde{\chi}_2^0 \to \tilde{\chi}_1^0 l^+ l^-)$. Notice that the branching ratio does not bound $\tan\beta$ by itself unless $Br(\tilde{\chi}_2^0 \to \tilde{\chi}_1^0 l^+ l^-) > 10\%$. The shapes of these contours are not particularly correlated to the constraint from the m_{ll} distribution shown in Fig. 7(a); therefore combining the two pieces of information might constrain the parameter space further. However, we should be aware that the branching ratio depends on the whole sfermion mass spectrum. For example, if there is a substantial reduction of masses for third generation sfermions, the branching ratio will be changed. Fits using the m_{ll} distribution are very important in that sense, because the shape depends only on ino mass parameters and $m_{\tilde{l}}$. Notice also that we only measure the sum of the products of several branching ratios rather than $Br(\tilde{\chi}_2^0 \to \tilde{\chi}_1^0 l^+ l^-)$ itself at the LHC.

5 Discussion and Conclusion

In this paper, we examined the impact of neutralino decay distributions on the study of the minimal supersymmetric standard model at the CERN LHC. The leptonic three body decay of the second lightest neutralino, $\tilde{\chi}_2^0 \to l^+l^-\tilde{\chi}_1^0$, is known to be very important because the end point of the lepton invariant mass distribution $m_{ll}^{\max}$ gives us direct information about the mass difference between $\tilde{\chi}_2^0$ and $\tilde{\chi}_1^0$, which gives us a stringent constraint on MSSM parameters.

We found that the neutralino decay distribution depends on the slepton masses rather sensitively. Measuring the shape of the lepton invariant mass distribution can be important even for the determination of $m_{ll}^{\max}$. In some cases, the measured end point may not coincide with the neutralino mass difference $m_{\tilde{\chi}_2^0} - m_{\tilde{\chi}_1^0}$, due to the strong suppression of the amplitude near $m_{ll}^{\max}$, while the leptonic branching ratio is still around a few %.

On the other hand, if systematic errors can be removed, the distribution gives us a model independent probe of the slepton mass scale. For the $\tilde{\chi}_2^0$ signal from $\tilde{g}$ decay, the S/N ratio is very large, or the background can be subtracted by using lepton pairs with opposite charge and different flavors. The remaining distribution can be further studied by looking at (A) the $\vec{\beta}_{\tilde{\chi}_2^0}$ distribution measured by using events which have m_{ll} near its end point, and (B) the lepton transverse momentum asymmetry A_l^T distribution, which is well correlated with the lepton energy asymmetry in the $\tilde{\chi}_2^0$ rest frame.

Notice that if the $\tilde{\chi}_2^0$ momentum distribution is precisely measured, leptonic decay distributions may be discussed without any QCD uncertainty, which might otherwise be substantial. Of course, the correlation with other cuts (e.g., on $\not{E}_T$, $\sum E_T$, lepton isolation) must be either small or determined from direct measurements, so that measurements in the lab frame allow us to reconstruct the $\tilde{\chi}_2^0$ decay distribution in its rest frame. The revenue of such an effort to reduce the uncertainty from the cuts is information on slepton masses and neutralino mixings, independent of any assumption about the mechanism to break supersymmetry.

In order to see if a study in such a direction is possible, dedicated MC simulations are necessary. Notice that the commonly available MC codes ISAJET and SPYTHIA used to simulate the three body decay distribution in phase space approximation. Our results show that a more careful treatment of $\tilde{\chi}_2^0 \to l^+l^-\tilde{\chi}_1^0$ decays is important, if one is interested in decay distributions. Moreover, the acceptance of such di-lepton events depends on the lepton energy in $\tilde{\chi}_2^0 \to l^+l^-\tilde{\chi}_1^0$ decays.

The study of $\tilde{\chi}_2^0$ decays can be easily done at e^+e^- colliders. $\tilde{\chi}_2^0\tilde{\chi}_2^0$ pair production or $\tilde{\chi}_2^0\tilde{\chi}_1^0$ co-production do not suffer from large backgrounds. Though the statistics is rather limited there, it would give us constraints on slepton masses and neutralino mixings. Notice that in supergravity models the lighter chargino and neutralinos are expected to be lighter than squarks and gluinos. Both LC and LHC may find and study $\tilde{\chi}_2^0$, and the information gleaned from these analyses can be combined to obtain a better understanding of MSSM parameters and the SUSY breaking mechanism.

Acknowledgements

We thank S. Kiyoura for earlier collaboration and discussion, H. Baer on the information about most recent ISAJET status, and M. Drees and X. Tata for comments and careful reading of manuscript. This work was supported in part by the Grant-in-Aid for Scientific Research (10140211 and 10740106) from the Ministry of Education, Science, Sports, and Culture of Japan. Y.Y. was also financially supported in part by Fuuju-kai Foundation.

Appendix

We show the explicit forms of the neutralino couplings used in section 2.

The neutralino mass matrix M_N in the gauge eigenbasis $(\tilde{B}, \widetilde{W}^3, \tilde{H}_1^0, \tilde{H}_2^0)$ is written as

$$M_N = \begin{pmatrix} M_1 & 0 & -m_Z c_\beta s_W & m_Z s_\beta s_W \\ 0 & M_2 & m_Z c_\beta c_W & -m_Z s_\beta c_W \\ -m_Z c_\beta s_W & m_Z c_\beta c_W & 0 & -\mu \\ m_Z s_\beta s_W & -m_Z s_\beta c_W & -\mu & 0 \end{pmatrix}, \tag{A1}$$

where $s_W = \sin\theta_W$, $c_W = \cos\theta_W$, $s_\beta = \sin\beta$, and $c_\beta = \cos\beta$. The mass eigenstates $\tilde{\chi}_i^0$ $(i = 1-4)$ are related to the gauge eigenstates via the mixing matrix N_{ij} as

$$\tilde{\chi}_i^0 = N_{i1}\tilde{B} + N_{i2}\widetilde{W}^3 + N_{i3}\tilde{H}_1^0 + N_{i4}\tilde{H}_2^0. \tag{A2}$$

We neglect the possibility of CP violation for sparticles and take N_{ij} as a real matrix by allowing negative values of $m_{\tilde{\chi}^0}$ in Eq. (4).

The interaction Lagrangian of fermion-sfermion-neutralino and neutralino-Z^0 couplings is written as

$$\mathcal{L}_{\rm int} = -g_2\overline{\tilde{\chi}_A^0}(a_{AX}^f P_L + b_{AX}^f P_R) f \tilde{f}_X^\dagger + ({\rm H.c.}) + \frac{g_Z}{2} z_{BA}^{(\tilde{\chi}^0)} \overline{\tilde{\chi}_B^0}\gamma^\mu\gamma_5\tilde{\chi}_A^0 Z_\mu^0, \tag{A3}$$

where f stands for l, ν, d, and u. The couplings $(a,\, b)$ for leptons are, in the $(\tilde{l}_L,\, \tilde{l}_R)$ basis,

$$\begin{aligned} a^l_{AX} &= \frac{1}{\sqrt{2}}\left\{[-N_{A2} - N_{A1}t_W]\delta_{X,L} + \frac{m_l}{m_W c_\beta}N_{A3}\delta_{X,R}\right\}, \\ b^l_{AX} &= \frac{1}{\sqrt{2}}\left\{\frac{m_l}{m_W c_\beta}N_{A3}\delta_{X,L} + 2N_{A1}t_W\delta_{X,R}\right\}, \\ a^\nu_{AX} &= \frac{1}{\sqrt{2}}[N_{A2} - N_{A1}t_W]\delta_{X,L}, \\ b^\nu_{AX} &= 0, \end{aligned} \tag{A4}$$

where $t_W = \tan\theta_W$. We have always ignored $\mathcal{O}(m_l)$ terms in Eq. (A4) in our numerical calculations.

The coupling of $\tilde{\chi}^0$ and Z^0 takes the form

$$z^{(\tilde{\chi}^0)}_{BA} = N_{B3}N_{A3} - N_{B4}N_{A4}. \tag{A5}$$

References

[1] JLC Group, JLC-1, KEK Report No. 92–16 (1992).

[2] T. Tsukamoto, K. Fujii, H. Murayama, M. Yamaguchi, and Y. Okada, Phys. Rev. D **51**, 3153 (1995).

[3] J. L. Feng, M. E. Peskin, H. Murayama, and X. Tata, Phys. Rev. D **52**, 1418 (1995).

[4] H. Baer, R. Munroe, and X. Tata, Phys. Rev. D **54**, 6735 (1996); D **56**, 4424(E) (1997).

[5] M. M. Nojiri, K. Fujii, and T. Tsukamoto, Phys. Rev. D **54**, 6756 (1996).

[6] H.-C. Cheng, J. L. Feng, and N. Polonsky, Phys. Rev. D **56**, 6875 (1997); D **57**, 152 (1998);
M. M. Nojiri, D. M. Pierce, and Y. Yamada, Phys. Rev. D **57**, 1539 (1998);
E. Katz, L. Randall, and S. Su, Nucl. Phys. B **536**, 3 (1999);
S. Kiyoura, M. M. Nojiri, D. M. Pierce, and Y. Yamada, Phys. Rev. D **58**, 075002 (1998).

[7] *New Directions for High-Energy Physics*, Proceedings of the 1996 DPF/DPB Summer Study on High-Energy Physics, Snowmass, Colorado, 1996, edited by D. G. Cassel, L. Trindle Gennari, and R. H. Siemann (SLAC, Stanford, 1997).

[8] I. Hinchliffe, F. E. Paige, M. D. Shapiro, J. Soderqvist, and W. Yao, Phys. Rev. D **55**, 5520 (1997).

[9] H. Baer, K. Hagiwara, and X. Tata, Phys. Rev. D **35**, 1598 (1987).

[10] I. Hinchliffe and F. E. Paige, hep-ph/9812233.

[11] M. Dine, A. E. Nelson, Y. Nir, and Y. Shirman, Phys. Rev. D **53**, 2658 (1996).

[12] J. Amundson *et al.*, Report of the Supersymmetry Theory subgroup, hep-ph/9609374, in Ref. [7].

[13] G. Dvali and A. Pomarol, Phys. Rev. Lett. **77**, 3728 (1996);
A. C. Cohen, D. R. Kaplan, and A. E. Nelson, Phys. Lett. B **388**, 588 (1996);
S. Dimopoulos and G. Giudice, Phys. Lett. B **357**, 573 (1995);
J. Hisano, K. Kurosawa, and Y. Nomura, Phys. Lett. B **445**, 316 (1999).

[14] H. Baer and X. Tata, Phys. Rev. D **47**, 2739 (1993).

[15] H. Baer, C. Chen, C. Kao, and X. Tata, Phys. Rev. D **52**, 1565 (1995).

[16] S. Mrenna, G. L. Kane, G. D. Kribs, and J. D. Wells, Phys. Rev. D **53**, 1168 (1996).

[17] S. Ambrosanio and B. Mele, Phys. Rev. D **53**, 2541 (1996).

[18] I. Iashvili and A. Kharchilava, Nucl. Phys. B **526**, 153 (1998).

[19] K. Griest, M. Kamionkowski, and M. Turner, Phys. Rev. D **41**, 3565 (1990);
M. Drees and M. M. Nojiri, Phys. Rev. D **47**, 376 (1993);
G. Jungman, M. Kamionkowski, and K. Griest, Phys. Rep. **267**, 195 (1996);
H. Baer and M. Brhlik, Phys. Rev. D **53**, 597 (1996).

[20] F. E. Paige, S. D. Protopopescu, H. Baer, and X. Tata, hep-ph/9810440.

[21] S. Mrenna, Comput. Phys. Commun. **101**, 232 (1997).

[22] S. Katsanevas and P. Morawitz, Comput. Phys. Commun. **112**, 227 (1998).

[23] Available at http://acfahep.kek.jp/subg/sim/softs.html.

[24] ECFA/DESY LC Physics Working Group, E. Accomando *et al.*, Phys. Rep. **299**, 1 (1998).

[25] Y. S. Tsai, Phys. Rev. D **4**, 2821 (1971);
T. Hagiwara, S.-Y. Pi, and A. I. Sanda, Ann. Phys. (N.Y.) **106**, 134 (1977);
A. Rougé, Z. Phys. C **48**, 75 (1990);
H. Kühn and F. Wagner, Nucl. Phys. **B236**, 16 (1984).

[26] B. K. Bullock, K. Hagiwara, and A. D. Martin, Phys. Rev. Lett. **67**, 3055 (1991); Phys. Lett. B **273**, 501 (1991); Nucl. Phys. B **395**, 499 (1993);
S. Raychaudhuri and D. P. Roy, Phys. Rev. D **52**, 1556 (1995).

[27] M. M. Nojiri, Phys. Rev. D **51**, 6281 (1995).

[28] R. Barbieri and L. J. Hall, Phys. Lett. B **338**, 212 (1994);
R. Barbieri, L. Hall, and A. Strumia, Nucl. Phys. B **445**, 219 (1995).

[29] M. Drees and M. M. Nojiri, Nucl. Phys. B **369**, 54 (1992).

[30] H. Baer, C-H. Chen, M. Drees, F. Paige, and X. Tata, Phys. Rev. Lett. **79**, 986 (1997); **80**, 642(E) (1998); Phys. Rev. D **58**, 075008 (1998); D **59**, 055014 (1999).

[31] J. D. Wells, Mod. Phys. Lett. A **13**, 1923 (1998);
V. Barger, C. Kao, and T.-J. Li, Phys. Lett. B **433**, 328 (1998);
V. Barger and C. Kao, hep-ph/9811489;
D. Denegri, W. Majerotto, and L. Rurua, hep-ph/9901231.

[32] H. Baer, C-H. Chen, F. Paige and X. Tata, Phys. Rev. D **54**, 5866 (1996).